

DEVELOPMENT OF A NUMERICAL MODEL FOR SUBCOOLED BOILING FLOW

J. Y. TU¹ and G. H. YEOH²

¹School of Aerospace, Mechanical and Manufacturing Engineering
RMIT University, Vic. 3083, Australia

²Australian Nuclear Science and Technology Organisation (ANSTO)
PMB 1, Menai, NSW 2234, Australia

ABSTRACT

Population balance equations combined with a three-dimensional two-fluid model are employed to predict bubbly flows with the presence of heat and mass transfer processes. Subcooled boiling flow belongs to this specific category of bubbly flows is considered. The MUSIG (MUltiple-Size-Group) model implemented in CFX4.4 is further developed to account for the wall nucleation and condensation in the subcooled boiling regime. Comparison of model predictions against local measurements near the test channel exit is made for the radial distribution of the bubble Sauter diameter, void fraction and gas and liquid velocities covering a range of different mass and heat fluxes and inlet subcooling temperatures. Additional comparison using empirical relationship to determine the local bubble diameter adopted in CFX4.4 boiling model is also investigated. Good agreement is better achieved with the local radial bubble Sauter diameter, void fraction and liquid velocity profiles against measurements using the newly formulated MUSIG boiling model over the simpler boiling model of CFX4.4. However, significant weakness of the model is still evidenced in the prediction of the vapour velocity. Work is in progress to circumvent the deficiency of the model by the consideration of an algebraic slip model to account for bubble separation.

INTRODUCTION

The capability to predict void fraction profiles and other two-phase flow parameters in subcooled boiling flows is of considerable importance to nuclear reactor safety and of great interest to many process industries. Two-phase turbulent bubbly flows with heat and mass transfer (subcooled boiling flows belong to this specific category of bubbly flows) are encountered in many industrial applications. Bubble column reactors are extensively employed for handling processes that require large interfacial area for gas-liquid mass transfer and efficient mixing of competing gas-liquid reactions (oxidations, hydrogenations, halogenations, aerobic fermentations, etc.) that are commonly found in many chemical, petroleum, mining, food and pharmaceutical industries. Engineering systems such as industrial boilers and heat exchangers also widely employ the two-phase mixture of liquid and vapour medium for either power generation or efficient removal of extensive heat generation.

Application of the *population balance approach* towards better describing and understanding complex industrial flow systems has received an unprecedented attention and acceptance. A population balance of any system concerns with maintaining a record for the number of entities,

which for bubbly flows, bubbles, or drops, whose presence or occurrence may dictate the behaviour of the system under consideration. In addition to the motion of these entities through the state space, it is usual to encounter "birth" processes that create new entities and "death" processes that destroy existing ones. The birth and death processes may depend on the states of the entities created or destroyed with an associated phenomenology; coalescence, breakage etc. are examples of such processes. A population balance model is, therefore, formulated based on the collective phenomenology contained in the displacement of entities through their state space and the birth and death processes that terminate entities and produce new entities.

With the advancement of computer technologies, the quest for improved designs has paved the trend biased towards the use of numerical simulations. Numerical methods are gradually gaining acceptance as a powerful tool for design of chemical reactors. Several studies have been conducted using the computational fluid dynamics (CFD) methodology (Krishna et al., 1999, Shimizu et al., 2000, Pohorecki et al., 2001, Olmos et al, 2001). The use of CFD and population balance models has shown to expedite a more thorough understanding of different flow regimes and further enhance the description of the bubble characteristics in the column volume for design, especially with the consideration of bubble coalescence and break-up mechanisms in the model simulations. Recently, Ramkrishna and Mahoney (2002) have highlighted a promising future towards handling two-phase flow systems using the *population balance approach*.

Interest in the precise prediction of two-phase flow behaviours in subcooled flow boiling is of great importance to the safety analysis of nuclear reactors. Many years of extensive research work have been performed with the aim of developing and verifying various thermal-hydraulics codes, such as, TRAC, CATHARE, ATHLET and RELAP5 or its recent extension RELAP5-3D. Nevertheless, it is still not possible to apply the existing boiling models developed in these codes, which were principally developed for power reactors, to perform safety analyses for research reactors without additional developments and extensions due to the specific features of the latter.

In the two-fluid model, which is the most commonly used macroscopic formulation of the thermo-fluid dynamics of the two-phase systems, the phasic interaction term appears in the field equations. These terms represent the mass, momentum and energy transfers through the interface

between the phases. An accurate determination of the bubble Sauter diameter is crucial as the bubble size influences the inter-phase heat and mass transfer through the interfacial area concentrations and momentum drag terms. Another consideration dominating the boiling process as observed in Lee et al. (2002) is the occurrence of large bubbles due to the competing mechanisms of bubble coalescence and condensation. The importance of coalescence and break-up of bubbles in bubble column reactors has been studied rather extensively through *population balance approach* in recent times due to the improved computer resources. Along similar development of models to consider bubble coalescence and break-up processes, a transport equation for the interfacial area has been considered by Kocamustafaogullari and Ishii (1995), Wu et al. (1998) and Hibiki et al. (2002) to handle two-phase turbulent bubbly flows. Here, the approach is to treat the bubbles as multiple type of groups not as a number of subdivided bubble classes having different discrete diameters covering the range of bubble sizes in the column volume. In an attempt to predict the transition of bubbly to slug or churn-turbulent flow regimes, Hibiki and Ishii (2000) proposed a two-group interfacial transport equations, which accounted bubbles belonging to spherical/distorted bubble group and cap/slug bubble group.

Although considerable efforts have been invested to develop more sophisticated models for bubble migration, attention of the transport processes is still very much focused on isothermal bubbly flow problems. Such flows greatly simplify the formulation of mathematical models where the heat and mass transfer processes can be safely neglected. In a boiling flow, heterogeneous bubble nucleation occurs within small pits and cavities at the heated surface where these nucleation sites are activated when the temperature of the surface exceeds the saturation temperature of the liquid at the local pressure. Bubbles subsequently detach from the heated surface due to the forces acting on them in the axial and normal directions, which include buoyancy, drag, lift, surface tension, capillary force pressure force, excess pressure force and the inertia of the surrounding liquid. If, at the same location, the temperature of the bulk fluid remains below saturation, the process is known as subcooled flow boiling. Because the bulk liquid remains mainly subcooled, bubbles migrated from the heated surface are condensed and the rate of collapse is dependent on the extent of the liquid subcooling. The interfacial contribution between the vapour and liquid due to heat and mass are characterised by temperature difference (subcooling), wall nucleation and condensation respectively. Subcooled boiling flows therefore behave

very differently from isothermal bubbly flows though a number of boiling experiments have confirmed some similarities in particular the presence of coalescence and break-up of bubbles inherently evidenced in both.

Experimentally, there has been an enormous interest in understanding the complex processes associated with bubbly flows with heat and mass transfer such as subcooled boiling flows. These experiments (Zeitoun and Shoukri, 1996, Bonjour and Lallemand, 2001, Prodanovic et al., 2002, Lee et al., 2002, Gopinath et al., 2002) have shed light to some interesting detail information on local bubble behaviour and size along the boiling channel volume. Observations made during experiments using high-speed photography (see Figure 1) revealed that large bubble sizes were present away from the heated wall not at the heated geometric boundary. The vapour bubbles, relatively small when detached from the heated surface, were seen to increase in size due to bubble coalescence confirming the observations of Prodanovic et al. (2002). As they migrated towards the centre of the flow channel, their sizes decreased due to the increased condensation as they migrated towards the opposite end of the unheated wall of the annular channel. This was further confirmed by experimental observations of Gopinath et al. (2002) (Figure 2), which illustrates a bubble gradually being condensed in a subcooled liquid away from the heated surface. Key observations are the significant coalescence visualised near the heater wall and condensation towards the unheated side. Also, detached bubbles originated from the surface cavities were found sliding or traveling close to the surface of the heater causing more coalescence. These fundamental observations have not been well modelled.

In our comprehensive review on axial void fraction distribution in channels, good agreement has been achieved against a wide range experimental data by improvements made to the boiling flow model in the generic CFD code - CFX4.4 (Tu and Yeoh, 2002). Further investigation in Yeoh et al. (2002) revealed significant weakness of the model predictions against local radial measurements of Lee et al. (2002) for subcooled boiling flow. This was evidenced in the prediction of bubble size distribution, local void fraction and liquid and vapour velocities. It was concluded that the determination of the local bubble size based only on the local liquid subcooling and pressure was insufficient to accurately represent the bubble coalescence and condensation. In the two-fluid approach as aforementioned, the phasic interaction term appears in the field equations. These terms represent the

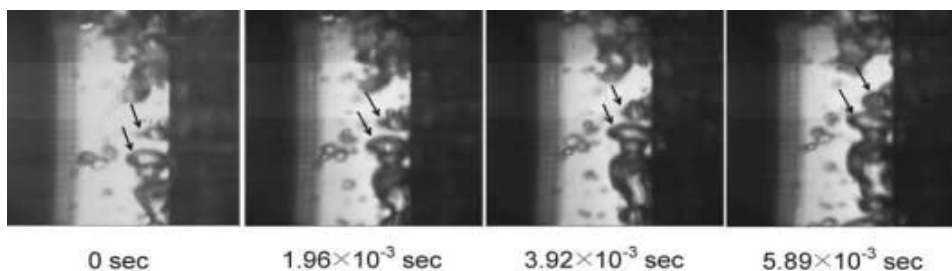


Figure 1: Significant bubble coalescence observed in the vicinity of the heated wall of an annular channel (Lee et al., 2002).

mass, momentum and energy transfers through the interface between the phases. Hence, an accurate determination of the bubble size distribution due to the significant presence of bubble coalescence and condensation in subcooled boiling flows is crucial as the bubble size influences the inter-phase heat and mass transfer and momentum terms. This important issue will be addressed in the current paper.

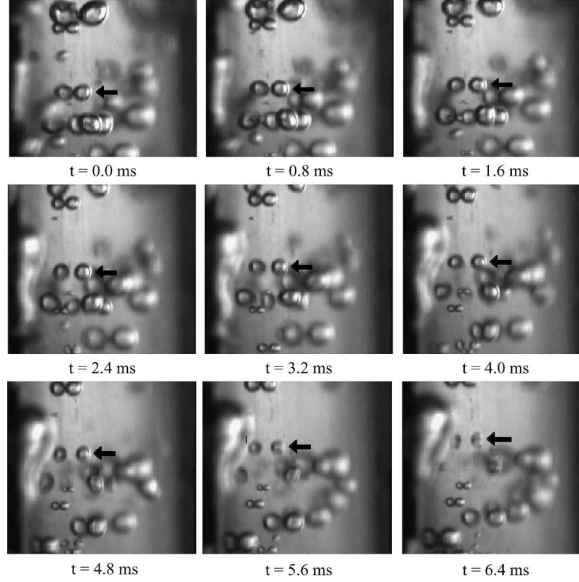


Figure 2: A bubble undergoing condensation in a subcooled liquid (Gopinath et al, 2002).

MODEL DESCRIPTION

Flow equations

The two-fluid model treating both the vapour and liquid phases as continua solves two sets of conservation equations governing mass, momentum and energy, which are written for each phase as:

Continuity Equation for Liquid Phase

$$\frac{\partial \rho_l \alpha_l}{\partial t} + \nabla \cdot (\rho_l \alpha_l \bar{u}_l) = \Gamma_{lg} \quad (1)$$

Continuity Equation for Vapour Phase

$$\frac{\partial \rho_g \alpha_g f_i}{\partial t} + \nabla \cdot (\rho_g \alpha_g \bar{u}_g f_i) = S_i - f_i \Gamma_{lg} \quad (2)$$

Momentum Equation for Liquid and Vapour Phases

$$\begin{aligned} & \frac{\partial \rho_k \alpha_k \bar{u}_k}{\partial t} + \nabla \cdot (\rho_k \alpha_k \bar{u}_k \bar{u}_k) = -\alpha_k \nabla P + \alpha_k \rho_k \bar{g} \\ & + \nabla \cdot \left[\alpha_k \mu_k^e (\nabla \bar{u}_k + (\nabla \bar{u}_k)^T) \right] \\ & + \sum_{j=1, j \neq k}^2 (\Gamma_{kj} \bar{u}_j - \Gamma_{jk} \bar{u}_k) + \sum_{j=1, j \neq k}^2 F_{kj} \quad (kj = lg; jk = gl) \end{aligned} \quad (3)$$

Energy Equation for Liquid and Vapour Phases

$$\begin{aligned} & \frac{\partial \rho_k \alpha_k H_k}{\partial t} + \nabla \cdot (\rho_k \alpha_k \bar{u}_k H_k) = Q_k \\ & + \nabla \cdot \left[\alpha_k \lambda_k^e \nabla T_k \right] + \sum_{j=1, j \neq k}^2 (\Gamma_{kj} H_j - \Gamma_{jk} H_k) \quad (kj = lg; jk = gl) \end{aligned} \quad (4)$$

In Eq. (1), Γ_{lg} represents the mass transfer rate due to condensation in the bulk subcooled liquid, which is expressed by

$$\Gamma_{lg} = \frac{h a_{if} (T_{sat} - T_l)}{h_{fg}} \quad (5)$$

where h is the inter-phase heat transfer coefficient determined from Ranz and Marshall (1952) Nusselt number correlation and a_{if} is the interfacial area per unit volume. The wall vapour generation rate is modelled in a mechanistic way derived by considering the total mass of bubbles detaching from the heated surface as:

$$\Gamma_{gl} = \frac{Q_e}{h_{fg} + C_{pl} T_{sub}} \quad (6)$$

where Q_e is the heat transfer due to evaporation. This wall nucleation rate is accounted in Eq. (2) as a specified boundary condition apportioned to the discrete bubble class based on the size of the bubble departure criteria on the heated surface. On the right hand side of Eq. (2), S_i is the source term due to coalescence and break-up based on the bubble coalescence and break-up model to be described later in the next section. The term $f_i \Gamma_{lg}$ represents the mass transfer due to condensation redistributed for each of the discrete bubble classes. The gas void fraction along with the scalar fraction f_i are related to the number density of the discrete bubble i th class n_i (similarly to the j th class n_j) as $\alpha_g f_i = n_i v_i$. The size distribution of the dispersed phase is therefore defined by the scalar f_i . The population balance equation for each of the discrete bubble classes n_i is provided in the next section. Inter-phase transfer terms in the momentum and energy equations – Γ_{kj} and F_{kj} – denote the transfer terms from phase j to phase k . The mass transfer Γ_{lg} is already given in Eq. (5) while the total interfacial force F_{lg} considered in the present study includes the effects of:

$$F_{lg} = \Gamma_{lg}^{drag} + F_{lg}^{lift} + \Gamma_{lg}^{lubrication} + \Gamma_{lg}^{dispersion} \quad (7)$$

where the terms on the right-hand side of Eq. (7) are the drag force, lift force, wall lubrication force and turbulent dispersion force respectively. Detailed expressions of these forces can be found in Anglart and Nylund (1996) and will not be repeated here. A k - ϵ turbulence model is employed for the continuous liquid and dispersed vapour phases. The effective viscosity in the momentum and energy equations is taken as the sum of the molecular viscosity and turbulent viscosity. The turbulent viscosity is considered as the total of the shear-induced turbulent viscosity and Sato's bubble-induced turbulent viscosity (Sato et al., 1981).

The wall heat flux Q_w can be divided into three components: heat transferred by conduction to the superheated layer next to the wall (nucleate boiling or surface quenching), Q_q ; heat transferred by evaporation or vapour generation, Q_e ; and heat transferred by turbulent convection, Q_c . Detailed expressions of these terms can be found in Tu and Yeoh (2002) and will not be repeated here.

The local bubble Sauter diameter based on the calculated values of the scalar fraction f_i and discrete bubble sizes d_i can be deduced from:

$$d_s = \frac{1}{\sum_i \frac{f_i}{d_i}} \quad (8)$$

Bubble coalescence and break-up model

The implementation of population balance equations originally developed by Lo (1996) for the generic computer code CFX4.4 is extended to account for the non-uniform bubble size distribution in the subcooled boiling flow regime. In this present study, bubbles ranging from 0 mm to 9.5 mm diameter are equally divided into 15 classes. Instead of considering 16 different complete phases, it is assumed that each bubble class travels at the same mean algebraic velocity to reduce the computational time. This therefore results in 15 continuity equations for the gas phase coupled with a single continuity equation for the liquid phase.

The break-up of bubbles in turbulent dispersions employs the model developed by Luo and Svendsen (1996). Binary break-up of the bubbles is assumed and the model is based on the theories of isotropic turbulence. For binary breakage, a dimensionless variable describing the sizes of daughter drops or bubbles (the breakage volume fraction) can be defined as

$$f_{BV} = \frac{v_i}{v} = \frac{d_i^3}{d^3} = \frac{d_i^3}{d_i^3 + d_j^3} \quad (9)$$

where d_i and d_j are diameters (corresponding to v_i and v_j) of the daughter bubbles in the binary breakage of a parent bubble with diameter d (corresponding to volume v). The value interval of the breakage volume fraction is between 0 and 1. The break-up rate of bubbles of volume v_j into volume sizes of $v_i (= v f_{BV})$ can be obtained as

$$\frac{\Omega(v_j : v_i)}{(1 - \alpha_g) n_j} = C \left(\frac{\varepsilon}{d_j^2} \right)^{1/3} \int_{\xi_{min}}^1 \frac{(1 + \xi)^2}{\xi^{11/3}} \exp \left(- \frac{12 c_f \sigma}{\beta \rho_l \varepsilon^{2/3} d_j^{5/3} \xi^{11/3}} \right) d\xi \quad (10)$$

where $\xi = \lambda/d_j$ is the size ratio between an eddy and a particle in the inertial sub-range and consequently $\xi_{min} = \lambda_{min}/d_j$; C and β are determined respectively from fundamental consideration of drops or bubbles breakage in turbulent dispersion systems to be 0.923 and 2.0 in Luo and Svendsen (1996); and c_f is the increase coefficient of surface area given by

$$c_f = \left[f_{BV}^{2/3} + (1 - f_{BV})^{2/3} - 1 \right] \quad (11)$$

The coalescence of two bubbles is assumed to occur in three steps. The first step involves the bubbles colliding thereby trapping a small amount of liquid between them. This liquid film then drains until it reaches a critical thickness and the last step features the rupturing of the liquid film subsequently causing the bubbles to coalesce.

The collisions between bubbles may be caused by turbulence, buoyancy and laminar shear. Only the first cause of collision (turbulence) is considered in the present model. Indeed collisions caused by buoyancy cannot be taken into account here as all the bubbles from each class have been assumed to travel at the same speed. Moreover, calculations showed that laminar shear collisions are negligible because of the low superficial gas velocities considered in this investigation. The coalescence rate considering turbulent collision taken from Prince and Blanch (1990) can be expressed as

$$\chi = \theta_{ij} \exp \left(- \frac{t_{ij}}{\tau_{ij}} \right) \quad (12)$$

where τ_{ij} is the contact time for two bubbles given by $(d_{ij}/2)^{2/3} / \varepsilon^{1/3}$ and t_{ij} is the time required for two bubbles to coalesce having diameter d_i and d_j estimated to be $\left\{ (d_{ij}/2)^3 \rho_l / 16 \sigma \right\}^{1/2} \ln(h_0/h_f)$. The equivalent diameter d_{ij} is calculated as suggested by Chesters and Hoffman (1982): $d_{ij} = (2/d_i + 2/d_j)^{-1}$. According to from Prince and Blanch (1990), for air-water systems, h_0 , initial film thickness and, h_f , critical film thickness at which rupture occurs are assumed to be 1×10^{-4} m and 1×10^{-8} m respectively. The turbulent collision rate θ_{ij} for two bubbles of diameter d_i and d_j is given by

$$\theta_{ij} = \frac{\pi}{4} [d_i + d_j]^2 (u_i^2 + u_j^2) \quad (13)$$

where the turbulent velocity u_i in the inertial sub-range of isotropic turbulence (Rotta, 1974) is:

$$u_i = 1.4 \varepsilon^{1/3} d^{1/3} \quad (14)$$

The general form for the population balance equation is

$$\frac{\partial n_i}{\partial t} + \nabla \cdot (\bar{u}_g n_i) = P_C + P_B - D_C - D_B - R_{ph} \quad (15)$$

where P_C , P_B , D_C and D_B are, respectively, the production rates due to coalescence and break-up and the death rate to coalescence and break-up of bubbles formulated as:

$$P_C = \frac{1}{2} \sum_{k=1}^N \sum_{l=1}^N \chi_{i,kl} n_k n_l$$

$$\chi_{i,kl} = \chi_{kl} \quad \text{if } v_k + v_l = v_i \quad \text{else } \chi_{i,kl} = 0 \quad \text{if } v_k + v_l \neq v_i$$

$$P_B = \sum_{j=i+1}^N \Omega(v_j : v_i) n_j \quad D_C = \sum_{j=1}^N \chi_{ij} n_i n_j \quad D_B = \Omega_i n_i \quad (16)$$

and R_{ph} denotes the source rate due to phase change, which for the present investigation is the collapse rate due to condensation for the subcooled boiling flow as aforementioned. The wall nucleation rate is not included

in R_{ph} and has been specified as a boundary condition as already described in the previous section.

EXPERIMENTAL DETAILS

The experimental-setup consists of a vertical concentric annulus with an inner heating rod of 19mm outer diameter. The heated section is a 1.67 m long Inconel 625 tube with 1.5 mm wall thickness and is filled with magnesium oxide powder insulation. The rod is uniformly heated by a 54 kW DC power supply. The outer wall is comprised of two stainless steel tubes with 37.5 mm inner diameter, which are connected by a transparent glass tube so that visual observation and taking photograph are made possible. The transparent glass tube is 50 mm long and is installed just below the measuring plane. The measuring plane is located at 1.61 m downstream of the beginning of the heated section. Demineralised water was used as the working fluid. More details regarding the experimental set-up can be found in Lee et al. (2002). The uncertainties of the void fraction and liquid and gas velocity measurements were approximated to be about 3%. However, the uncertainty of the bubble Sauter diameter values, applied equally to the interfacial area concentration, was difficult to ascertain and will, at present, be estimated to be lower than 27%. Experimental conditions that have been used for comparison with the simulated results are presented in Table 1. Figure 3 shows the schematic drawing of the test channel. θ_{sub} is defined as the difference between the saturation temperature T_{sat} and local temperature T .

Run	P_{inlet} [MPa]	T_{inlet} [°C]	θ_{sub} (inlet) [°C]	Q_w [kW/m ²]	G [kg/m ² s]
C1	0.142	96.6	13.4	152.3	474.0
C2	0.137	94.9	13.8	197.2	714.4
C3	0.143	92.1	17.9	251.5	1059.2

Table 1: Experimental conditions.

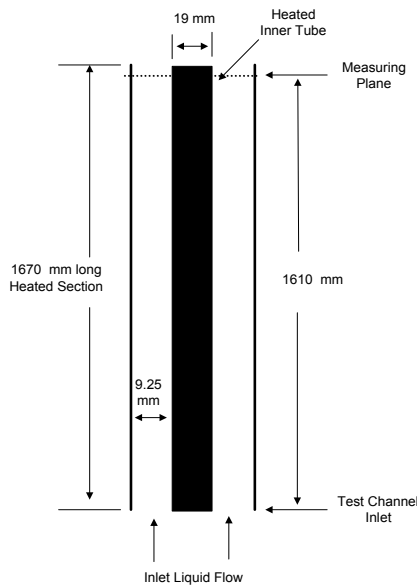


Figure 3: Schematic drawing of the test channel.

NUMERICAL DETAILS

Solution to the two sets of governing equations for the balance of mass, momentum and energy of each phase was sought. The discrete bubble sizes prescribed in the dispersed phase were further tracked by solving an additional set of 15 transport equations, which these equations were progressively coupled with the flow equations during the iteration procedure. The conservation equations were discretised using the control volume technique. The velocity-pressure linkage was handled through the SIMPLE procedure. The discretised equations were solved using Stone's Strongly Implicit Procedure Stone (1968). Since the wall heat flux was applied uniformly throughout the inner wall of the annular and taking advantage of the annular geometrical shape, only a quarter of the annular was considered as the domain for simulation. A body-fitted conformal system was employed to generate the three-dimensional mesh within the annular channel resulting in a total of 13 (radial) \times 30 (height) \times 3 (circumference) control volumes. Grid independence was examined. In the mean parameters considered, further grid refinement did not reveal significant changes to the two-phase flow parameters. Convergence was achieved within 1500 iterations when the mass residual dropped below 1×10^{-7} . Global execution time on the Silicon Graphics machine was about 30 minutes.

RESULTS AND DISCUSSION

The radial profiles of the bubble Sauter diameter, void fraction, interfacial area, vapour and liquid velocities located at 1.61 m downstream of the beginning of the heated section are predicted through the two-fluid and MUSIG boiling models. In all the figures presented, the dimensionless parameter $(r-R_i)/(R_o-R_i) = 1$ indicates the inner surface of the unheated flow channel wall while $(r-R_i)/(R_o-R_i) = 0$ indicates the surface of the heating rod in the annulus channel.

The MUSIG boiling model predictions against local measurements are further accompanied by computational results determined through an empirical relationship of Anglart and Nylund (1996) to determine the local bubble diameter. They have proposed to estimate the interfacial transfer terms through a bubble diameter relationship assuming a linear dependence with local liquid subcoolings, which it can be expressed by:

$$d = \frac{d_1(\theta_{sub} - \theta_0) + d_0(\theta_1 - \theta_{sub})}{\theta_1 - \theta_0} \quad (17)$$

This relationship is still currently being used and applied in many boiling studies through the CFX4.4 code. Application of this correlation for subcooled boiling flow at low pressures has recently reported in Lee et al. (2002) numerical investigations.

Reference diameters of d_0 and d_1 in Eq. (17) corresponding to the reference subcooling temperatures at θ_0 and θ_1 are usually not known *a priori*. Calculations based on difference reference diameters have been investigated in the present study. We have assumed for the first case - "Linear1" - the local bubble diameters were evaluated between $d_0 = 1.5 \times 10^{-4}$ m and $d_1 = 4.0 \times 10^{-3}$ m while for the second case - "Linear2" - they are determined between $d_0 = 1.5 \times 10^{-4}$ m and $d_1 = 7.0 \times 10^{-3}$ m respectively. We further

assumed that both of the reference diameters corresponded to identical reference subcooling temperatures of $\theta_0 = 13.0$ K and $\theta_1 = -5$ K.

Figure 4 illustrates the local radial bubble Sauter diameter distribution at the measuring plane of the heated annular channel. In all the three cases, the empirical correlations from Anglart and Nylund (1996) misrepresented the local bubble sizes. The gradual increase of the bubble Sauter diameters towards the heated wall with the highest bubble sizes predicted at the heated wall by the empirical relationships contradicted the local radial measurements. In the experiments, high-speed photography (see Figure 1) clearly demonstrated large bubble sizes were present away from the heated wall not at the heated wall. However, this trend was correctly predicted by the MUSIG boiling model. Good agreement was achieved against the measured bubble sizes for all the three experimental conditions. The predicted bubble diameter behaviour determined through the empirical correlation was deficient due to the absence of properly accommodating the bubble mechanistic behaviour coalescence and collapse due to condensation, which was succinctly observed in experiments. Evidently, the bubble size determination in the bulk liquid core was not strictly dependent on only local subcoolings. This relationship was seen to significantly compromise the model predictions. Extending the use of this bubble diameter correlation to predict local bubble sizes is invalid.

It was also observed in Lee et al. (2002) that the vapour bubbles, relatively small when detached from the heated surface, increased in size due to bubble coalescence as they migrated towards the centre of the flow channel. The bubble departure diameter evaluated from the wall heat partition model resulted in a bubble size of approximately 1.8 mm. In all the three cases, a maximum predicted bubble size for C1, C2 and C3 of about 4.5 mm, 4.0 mm and 3.8 mm respectively confirmed the experimental observations. It was also interesting to note that coalescence of bubbles occurred axially along the heated surface. Experiments by Bonjour and Lallemand (2001) and Prodanovic et al. (2002) have clearly indicated the presence of bubbles sliding shortly after being detached from the heated surfaces before lifting into the liquid core. These upstream bubbles travelling closely to the heated wall have the tendency of significantly colliding with any detached bubbles downstream and subsequently forming bigger bubbles due to the bubbles merging together. Here, simulations have determined a bubble Sauter diameter of 3 mm corresponding to the adjacent points along the heated wall for all the three experimental conditions C1, C2 and C3. The bubble sizes being substantially larger than the bubble departure diameter have demonstrated to some degree the capability of the MUSIG boiling model to capture the coalescence behaviour of the bubbles sliding along the heated surface.

As the bubbles migrated towards the opposite end of the adiabatic wall, they are decreased due to the increased condensation. Here, only the *low-temperature* single-phase subcooled water existed. The bubble Sauter diameter profiles of the MUSIG boiling model clearly showed the gradual collapse of the bubbles and the absence of bubbles near the adiabatic wall of the test channel. Important insights to the effect of condensation

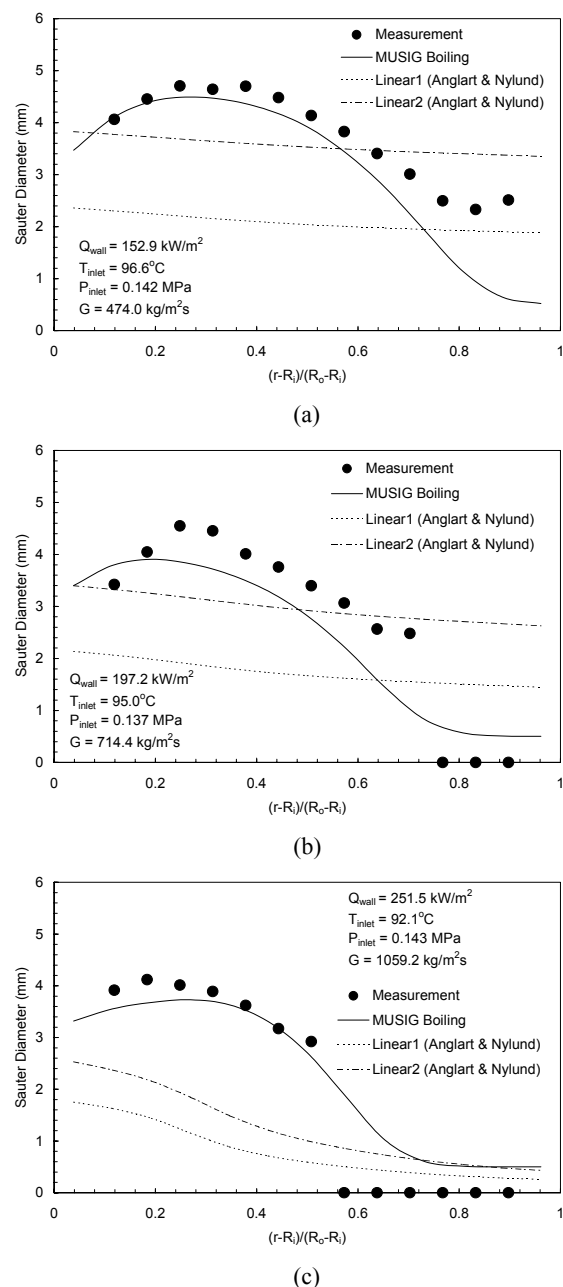


Figure 4: Local mean radial profiles of bubble Sauter diameter: (a) C1, (b) C2 and (c) C3.

revealed that more bubbles were condensed with a higher inlet subcooling condition as shown in Figure 4(c) and with increasing mass fluxes, interfacial heat transfer was further enhanced thereby resulting in more bubbles being condensed in the subcooled liquid core.

Figure 5 presents the locally predicted void fraction profiles against radial measured values. The peak local void fraction was always observed in the vicinity of the heated surface in a typical subcooled boiling flow. This high local void fraction found here was explicitly due to the large number of bubbles generated from the active nucleation sites on the heated surface. Here, large amount of bubbles was generated from these nucleation sites when the temperature on the heated surface exceeded the saturation temperature. As these bubbles reached a critical size, they detached and migrated laterally toward the subcooled liquid core under the

competing process of bubble coalescence and condensation as aforementioned.

The use of “Linear1” reference diameters in Eq. (17) significantly underpredicted the local void fraction distribution for all the experimental conditions. By employing a larger reference diameter of d_l in “Linear2”, the predictions fared better. Albeit its simplicity formulation and application, the use this relationship failed to offer any significant benefits due to the *ad hoc* specifications of its reference diameters. In some boiling problems, the setting of proper reference subcooling limits needs revision, which are also not known *a priori*. More importantly, extending the use of this empirical relationship for other types of boiling flow regimes may not be confidently applied beyond the subcooled bubbly flow regime, the changes in the two-phase flow structures from bubbly to slug or churn turbulent boiling flows, and other geometries. Nevertheless, the MUSIG boiling model (fundamentally derived from population balance principles) has the capacity of accommodating the different range of bubble sizes and mechanisms that may be present within the boiling liquid. It therefore presents enormous potential of possibly tracking the transition from one flow regime to another and mechanistically predicting the bubble sizes associated for each of the boiling flow regimes. This approach may well replace traditional flow regime maps and regime transition criteria. For example, numerical studies of adiabatic bubbly flows in bubble columns conducted through Olmos et al. (2001) have demonstrated the capability of the MUSIG model to predict the evolution of bubble sizes between two domains. In these two domains, the characteristics of the bubbles are typical of the homogeneous and transition regimes.

The radial profiles of the axial component of the local vapour velocity are shown in Figure 6 while Figure 7 presents the radial profiles of the local liquid velocity for experimental conditions C1, C2 and C3. The vapour velocity was greater than the liquid velocity due to buoyancy force caused by density difference. As was observed in the experiment, the vapour velocity was higher at the centre than the velocities near the heating rod. This was probably due to the buoyancy effect being enhanced for the migration of the large bubbles there, which was again confirmed by high-speed photography in Lee et al. (2002). However, the vapour velocity predicted by the MUSIG boiling model along with local empirical bubble diameter relationship for calculating the local bubble sizes showed that higher velocity values approaching the heated boundary. The MUSIG boiling model vapour velocities in the vicinity of the heated surface were rather similar to those of the simpler models for all the three cases because of the assumption that each bubble class travelled at the same mean algebraic velocity. The philosophy behind adopting this approach for the subcooled boiling studies was to hasten the computational time and reduce computational resources. However, the large discrepancies between the predicted and measured velocities near the heated wall demonstrated the inadequacy of the adopted approach. Within the channel space, different size bubbles are expected to travel with different speeds. As a first step towards resolving the problem, an algebraic slip model is proposed to account for bubble separation. The terminal velocities for each of

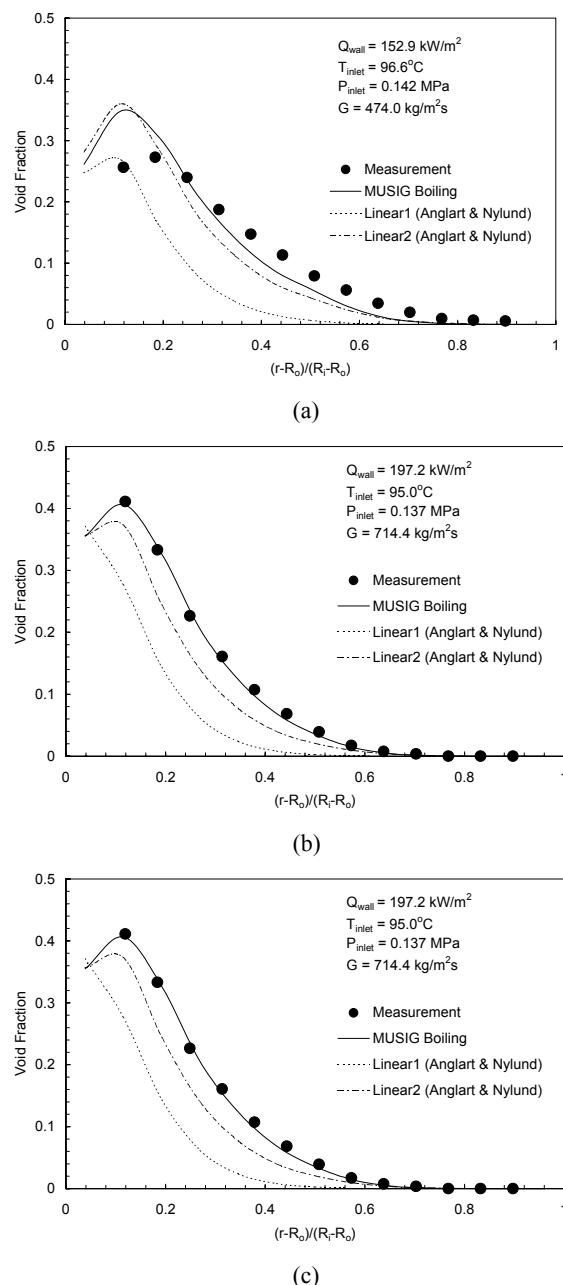
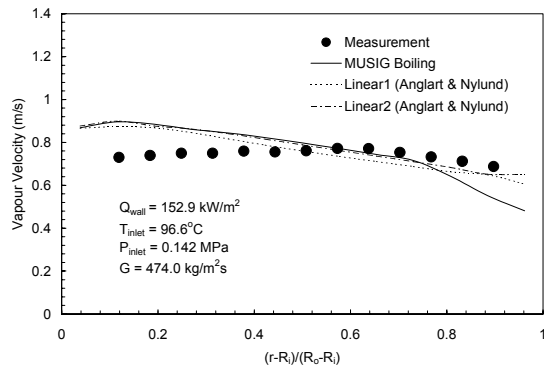
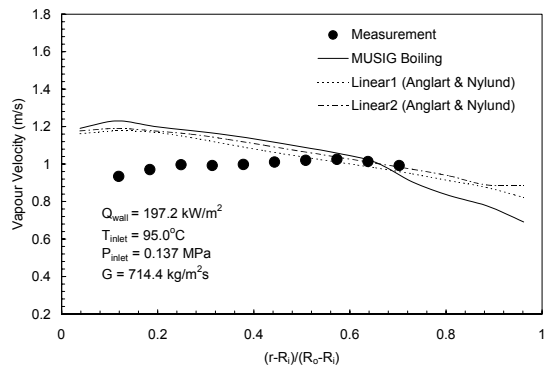


Figure 5: Local mean radial profiles of void fraction: (a) C1, (b) C2 and (c) C3.

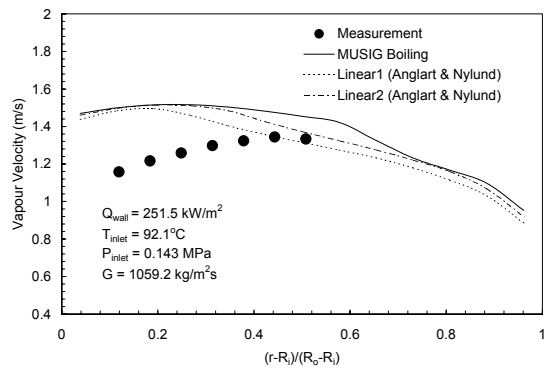
the bubbles can be considered through applying an algebraic relationship suggested by Clift et al. (1978), which are then used to evaluate the individual bubble slip velocities. Work is currently in progress to overcome this deficiency of the two-fluid and MUSIG boiling models with the development of an algebraic slip model so that bubble separation can be considered resulting in proper evaluation of slip velocities. Nevertheless, in Figure 7, good agreement achieved for the liquid velocities between the predictions and experimental values at the measuring plane in the liquid phase was gratifying. These velocities showed a closer resemblance to the measurements than the predicted profiles of the vapour velocity.



(a)



(b)

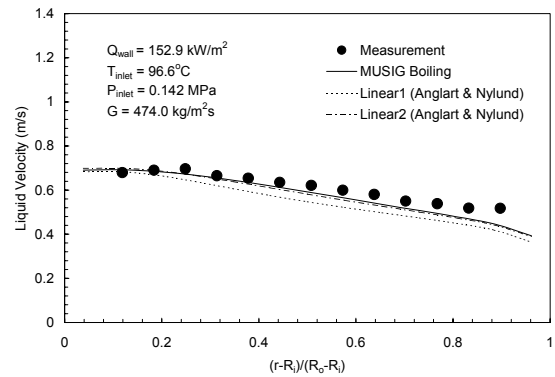


(c)

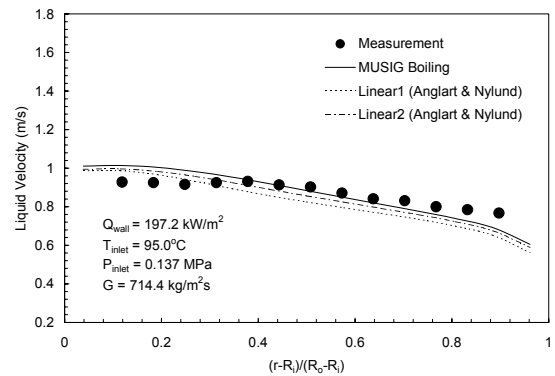
Figure 5: Local mean radial profiles of vapour velocity: (a) C1, (b) C2 and (c) C3.

CONCLUSION

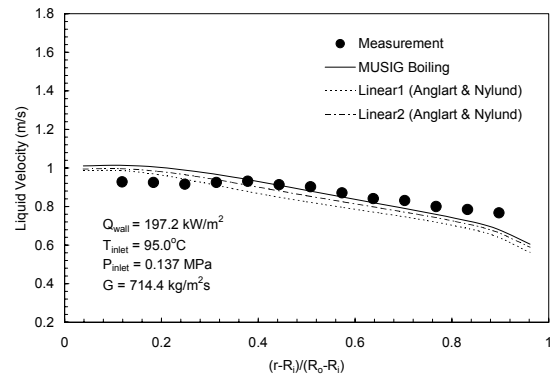
A two-fluid model coupled with population balance approach is presented in this paper to handle bubbly flows with the present of heat and mass transfer processes. The increase in complexity of modelling such flows derives from the additional consideration of the gas or liquid undergoing a phase transformation. Subcooled boiling flow belongs to a specific category of bubbly flows with heat and mass transfer where it embraces all the complex dynamic interaction of the phenomena associated with hydrodynamics, heat and mass transfer, and bubbles coalescence and break-up. Modelling subcooled boiling flows particularly at low pressures have been successfully demonstrated. The range of bubble sizes in the subcooled boiling flow was distributed according to the division of 15 diameter classes through the formulation of a MUSIG model. Each of them experiencing coalescence and break-



(a)



(b)



(c)

Figure 6: Local mean radial profiles of liquid velocity: (a) C1, (b) C2 and (c) C3.

up phenomena has been considered. The MUSIG boiling model was developed to account for the wall nucleation or vapour generation on the heated surface and condensation process in the subcooled liquid core combined with the bubble coalescence of Prince and Blanch (1990) and bubble break-up of Luo and Svendsen (1997). Comparison of the predicted results was made against recent local measurements of Lee et al. (2002). Additional comparison employing empirical relationship to determine the local bubble diameter adopted in CFX4.4 boiling model was also investigated. Good agreement was achieved through the newly formulated MUSIG boiling model for the local bubble Sauter diameter, void fraction, and liquid velocity profiles. However, in the gas phase, since the assumption was invoked where each bubble class travelled at the same mean algebraic velocity in order to reduce the computational time and resources, significant weakness of the model was evidenced in the prediction of the vapour

velocity. Research is currently ongoing to develop an algebraic slip model to account for bubble separation to yield a more realistic prediction of the vapour velocity.

REFERENCES

- ANGLART, H. and NYLUND, O., (1996), "CFD application to prediction of void distribution in two-phase bubbly flows in rod bundles", *Nucl. Sci. Eng.*, **163**, 81-98.
- BONJOUR, J. and LALLEMAND, M., (2001), "Two-phase flow structure near a heated vertical wall during nucleate pool boiling", *Int. J. Multiphase Flow*, **27**, 1789-1802.
- CHESTERS, A. K. and HOFFMAN, G., (1982), "Bubble coalescence in pure liquids", *Appl. Sci. Res.*, **38**, 353-361.
- CLIFT, R., GRACE, J. R. and WEBER, M. E., (1978), "Bubbles, Drops and Particles", Academic Press, New York.
- GOPINATH, R., BASU, N. and DHIR, V. K., (2002), "Interfacial heat Transfer during subcooled flow boiling", *Int. J. Heat Mass Transfer*, **45**, 3947-3959.
- HIBIKI, T., and ISHII, M., (2000), "Two-group area transport equations at bubbly-to-slug flow transition", *Nucl. Eng. Design*, **202**, 39-76.
- HIBIKI, T., and ISHII, M., (2002), "Development of one-group interfacial area transport equation in bubbly flow systems", *Int. J. Heat Mass Transfer*, **45**, 2351-2372.
- KOCAMUSTAFAOGULLARI, G. and ISHII, M., (1995), "Foundation of the interfacial area transport equation and its closure relations", *Int. J. Heat Mass Transfer*, **38**, 481-493.
- KRISHNA, R., URSEANU, M. I., VAN BATEN, J. M. and ELLENBERGER, J., (1999), "Influence of scale on the hydrodynamics of bubble columns operating in the churn-turbulent regime: experiments vs. Eulerian simulations", *Chem. Eng. Sci.*, **54**, 4903-4911.
- LEE, T. H., PARK, G.-C. and LEE, D. J., (2002), "Local flow characteristics of subcooled boiling flow of water in a vertical annulus", *Int. J. Multiphase Flow*, **28**, 1351-1368.
- LO, S., (1996), "Application of population balance to CFD modelling of bubbly flow via the MUSIG model", AEA Technology, *AEAT-1096*.
- LUO, H. and SVENDSEN, H., (1996), "Theoretical model for drop and bubble break-up in turbulent dispersions", *AIChE J.*, **42**, 1225-1233.
- OLMOS, E., GENTRIC, C. VIAL, CH., WILD G. and MIDOUX, N., (2001), "Numerical simulation of multiphase flow in bubble column reactors. Influence of bubble coalescence and break-up", *Chem. Eng. Sci.*, **56**, 6359-6365.
- PRODANOVIC, V., FRASER D. and SALCUDEAN, M., (2002), "Bubble behaviour in subcooled flow boiling of water at low pressures and low flow rates", *Int. J. Multiphase Flow*, **28**, 1-19.
- PRINCE, M. J. and BLANCH, H. W., (1990), "Bubble coalescence and break-up in air-sparged bubble column", *AIChE J.*, **36**, 1485-1499.
- RAMKRISHNA, D. and MAHONEY, A. W., (2002), "Population balance modeling. Promise for the future", *Chem. Eng. Sci.*, **57**, 595-606.
- RANZ, W. E. and MARSHALL, W. R., (1952), *Chem. Eng. Prog.*, **48**, 141-148.
- ROTTA, J. C. (1972). *Turbulente Stromungen*, B. G. Teubner, Stuttgart.
- POHORECKI, R., MONIUK, W., BIELSKI, P. and ZDROJKWOSKI, A., (2001), "Modelling of the coalescence/redispersion processes in bubble columns", *Chem. Eng. Sci.*, **56**, 6157-6164.
- SATO, Y., SADATOMI, M. and SEKOGUCHI, K., (1981), "Momentum and heat transfer in two-phase bubbly flow-I", *Int. J. Multiphase Flow*, **7**, 167-178.
- SHIMIZU, K., TAKADA, S., MINEKAWA, K. and KAWASE, Y., (2000), "Phenomenological model for bubble column reactors: prediction of gas hold-up and volumetric mass transfer coefficients", *Chem. Eng. J.*, **78**, 21-28.
- STONE, H. L., (1968), "Iterative solution of implicit approximations of multidimensional partial differential equations", *SIAM J. Num. Anal.*, **5**, 530-558.
- TU, J. Y. and YEOH, G. H., (2002), "On numerical modelling of low-pressure subcooled boiling flows", *Int. J. Heat Mass Transfer*, **45**, 1197-1209.
- WU, Q., KIM, S., ISHII, M., and BEUS, S. G., (1998), "One-group interfacial area transport in vertical bubbly flow", *Int. J. Heat Mass Transfer*, **41**, 1103-1112.
- YEOH, G. H., TU, J. Y., LEE, T. H. and PARK, G.-C., (2002), "Prediction and measurement of local two-phase flow parameters in a boiling flow channel", *Num. Heat Transfer, Part A: Applications*, **42**, 173-192.
- ZEITOUN, O. and SHOUKRI, M., (1996), "Bubble behaviour and mean diameter in subcooled flow boiling", *ASME J. Heat Transfer*, **118**, 110-116.

